PROTOTYPE MEASUREMENTS OF FLOW IN CASINGS OF PELTON TURBINES– MEASUREMENT SYSTEM, CALIBRATION AND RESULTS

Alexander Arch[1] & Dominik Mayr[2]

[1] Generation Technology Conventional / Hydro, EnBW-AG, Germany, Durlacher Allee 93 – 76131 Karlsruhe

[2] Generation High head plants, VERBUND Hydro Power AG, Austria, E-Werkstrasse 149, 8121 Deutschfeistritz

E-mail: a.arch@enbw.com, dominik.mayr@verbund.com

Abstract

In this paper results of prototype measurements are presented concerning the distribution of the flow just above the tailrace water level coming down from the Pelton wheel. The measurements have been realized by using a newly developed measuring technique based on pressure probes. The measurement system and calibration is described. The impact velocity of the water particles on the surface of the tailrace water, diameters of the droplets coming down from the runner and their distribution over the casing section are presented.

Introduction

Under special conditions the backpressure operation of Pelton turbines may represent an interesting alternative to common set-ups, but special knowledge on aeration and de-aeration along the tailwater is required.

In former research work, conducted at Graz University of Technology, Austria, the behaviour of the air-water mixture in the tailrace channel with respect to the distribution of the amount of air and the size of air bubbles was investigated. This work was done based on prototype measurements in three different plants. Results regarding the de-aeration processes have already been published (Arch & Mayr, 2006) and (Arch, 2008). Moreover, effects of the increased air density on the physical properties of the air-water mixtures due to the backpressure operation were studied (Arch & Mayr, 2006). To get a better insight into the hydrodynamic process additional tests on hydraulic / physical section models were done at the institute of hydraulic engineering and water resources management. Even though this former research work brought up important new findings, information about the geometry and energy of the water flow coming down from the Pelton runner is seen as the crucial boundary condition for estimating the amount of air initially entrained into the tailwater.

Not only due to the difficulty of reproducing the flow coming out from the rotating Pelton buckets but also to model the water flows, which are corresponding to the outflow of the several nozzles in the casing, laboratory tests were not seen suitable and effective to gain detailed knowledge about the flow processes in the casing. Moreover, turbulence effects due to the velocity reduction in the Pelton bucket are almost not reproducible in scale laboratory studies. Thus additional prototype measurements were undertaken along with detailed laboratory studies. Availing the opportunity to link the results in the casing with those from prototype measurements of the de-aeration process in the tailrace channel, the HEPP Koralpe was chosen due to easy access to the casing.

Prototype Measurements

Plant description

The salient features and the main section of the Koralpe hydropower plant are listed in table 1 and figure 2. Most notable for the process of air entrainment are the velocities c_2 at the exit of the bucket, which can be seen in figure 1. They were calculated using formulas from turbine design manuals.

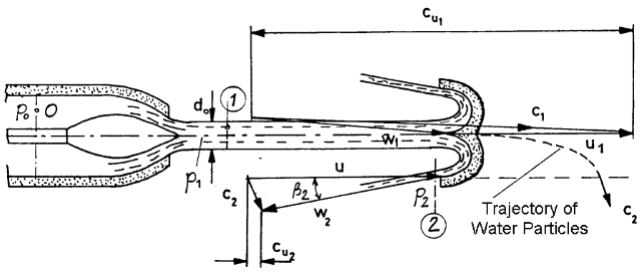

Figure 1: Pelton turbine, velocities at Pelton bucket

The exit-angle β_2 of the buckets is 7.1 degrees. Based on the net head of 720 m where all 6 nozzles are operating a jet-velocity directly at the nozzle of 116.5 m/s was calculated considering all hydraulic losses in the entire headrace system as well as in the spiral casing. Based on these assumptions the velocity of the flow at the exit of the bucket was estimated to c_2 = 6.5 to 7.1 m/s. The range of the velocity is explained by the variation of parameters cited in literature, which are used for the calculation and representing hydraulic losses in the bucket taking friction and turbulence effects into account. The change of the jet

velocity c_0 due to fluctuation of the water level in the reservoir is less than 1 % and thus can be neglected. Moreover, during the measurements the reservoir level was kept constant at design level.

Operating the turbine under rated conditions, approximately 70 to 80 % of the outer edge of the bucket is covered by the water flow. Assuming a constant width of the water layer a thickness of 1.7 to 2.5 cm of the exiting plane jet can be estimated. Based on these parameters and by applying the frictionless Bernoulli equation (1), a maximal impact velocity v_J at the water surface of the tailrace channel of 9.41 – 9.81 can be calculated by assuming a mean runner clearance f of 2.4 m. The variation of the velocity is referred to the differences of friction losses due to the varying length of the water in touch with the bucket while flowing through.

$$v_J = \sqrt{c_2^2 + 2gf} \qquad (1)$$

Measurement System

To gain information on the impact velocity and the flow distribution over the horizontal casing section of the water falling down from the runner in prototype installations represents a notable challenge with respect to the measurement equipment. Due to the lack of information where the water flow will come down from the runner during turbine start, high velocities (> 100 m/s) and hence high impact pressures had to be assumed on the selected equipment. Using pressure probes was finally decided to be the most suitable measurement technique. 14 pressure probes were arranged vertically, which allowed the vertical portion of the impact velocity to be measured. Optical systems or volume capturing methods as well as conductivity based measurements methods could not be applied due to required sampling rate of data acquisition and/or missing robustness.

In total 3,480 points - distributed over a rectangle of 2.5 times 2.3 m and 1.95 m below the jet level were measured under full load conditions by using a remote-controlled measurement device consisting of a moveable “transducer box” mounted on a rigid steel frame which was fixed on the inspection grid inside the casing.

Table 1: Salient features of the Power Plant Koralpe

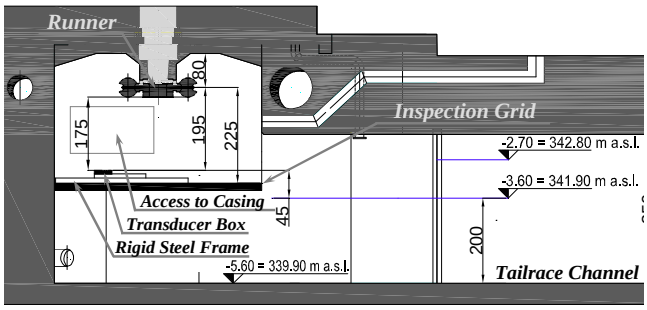

Figure 2: Section of the Casing and tailrace

To shorten up the acquisition time and to finish the prototype measurements within one week, 8 positions (lateral spacing 60.5 mm) were measured simultaneously with dynamic pressure probes and 6 positions/locations with absolute pressure probes. Therefore in 3/4th of the locations a measurement with both systems was conducted which allowed a detailed crosscheck and validation of the gained results afterwards. The start of one measurement was triggered with respect to the turbine position and thus always started at the same position of the buckets. Based on the equations for the potential and kinetic energy, the velocity v_J of a water particle of density ρ impacting on a rigid surface with pressure p can be theoretically related as follows:

$$v_J \sim \sqrt{\frac{2 \cdot p}{\rho}} \qquad (2)$$

Based on this approach the pressure corresponding to the real impact velocity had to be defined. As it can be seen in the descriptive figure 3, high speed camera measurements (HSC-measurements) were used to determine the velocity of falling water droplets onto a probe related to the measured pressure signals and hence calibrating the evaluation method. As can be seen in the figure, the signal of an impacting droplet is highly dynamic (in addition to having random characteristics).

In this context dozens of test runs with circular jets or droplets of different diameters were done by using different pressure probes. Due to the expected rough conditions in the casing, a solution was found by using dynamic (transducer PCB M112A22, D=5.52 mm) as well as static pressure probes (transducer AMP-550-M5-10bar, D=3.5 mm). The installation of two different systems

Rated Discharge Q_D	8	m³/s	Clearance	1.95 - 2.70	m
max. Discharge Q_{MAX}	9.3	m³/s	Nominal Runner Diameter	1450	mm
No. of Nozzles	6	-	Jet Velocity C_0	116.5	m/s
Q / Nozzle	1.33	m³/s	abs. Exit-Velocity C_2	6.50 - 7.10	m/s
Gross Head H_B	735.5	m	Vertical Portion of C_2 - $C_{2\,vert}$	6.45 - 7.06	m/s
Net Head H_N	720	m	Circumferental Speed U	56.94	m/s
Jet Diameter d_0	125	mm	Impact Velocity v_J at mean Clearance	9.41 - 9.81	m/s
Rated Speed n	750	rpm	No. of Buckets	21	[-]
Runaway Speed n_D	1330	rpm	Height of Bucket B_H	366.6	mm
Rated Power	50	MW	Width of Bucket B_B	395	mm
max. Power	55	MW	Depth of Bucket B_T	118.5	mm

should enable a crosscheck of the gained measurement values.

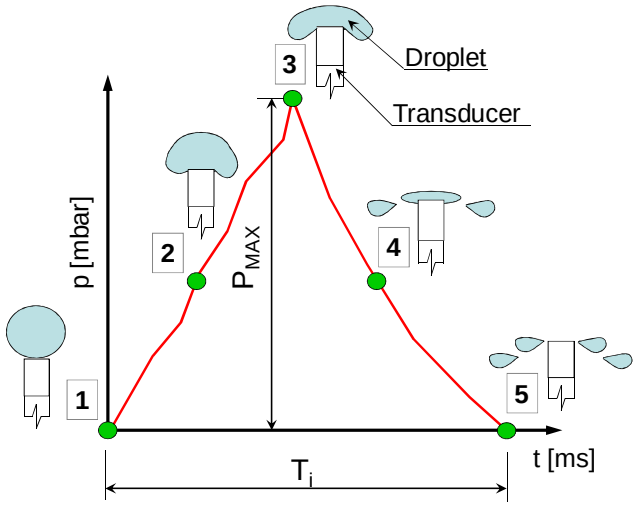

Figure 3: HSC-calibration measurements and descriptive graphic of the pressure transducer signal

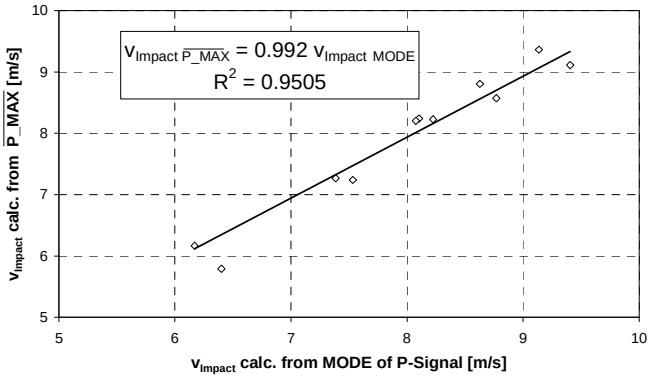

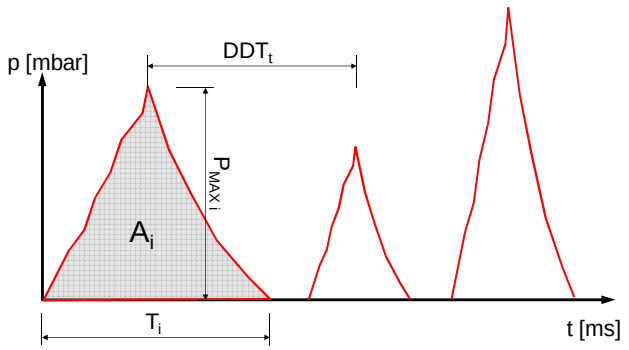

Figure 4: Comparison of the impact velocity based on equation (2) for absolute and equation (3) for dynamic pressure transducers (above) – definition of impact parameters (below)

During calibration of the entire measurement system for the static pressure probes it could be seen that the velocity of falling water particles as well as for continuous circular jets can be determined by using the mode of the recorded pressure signals which have to be measured with a scanning rate of at least 20 kHz in order for the results to be independent from the sampling frequency.

This was not valid for the dynamic probes due to their different construction and assembling. Therefore a different approach was found for calculating the impact velocity based on the maximal pressure measured for one particle as follows:

$$v_i = \sqrt{\frac{\overline{P_{MAX}}}{\rho}} \quad \text{where} \quad \overline{P_{MAX}} = \frac{\sum_{i=1}^{n} P_{MAX\,i}}{n} \qquad (3)$$

Wherein $\overline{P_{MAX}}$ [Pa] is the mean maximal pressure due to the impact of water droplets, ρ [kg/m³] is the density of water. By using these two approaches a correlation was found for the two different measurement systems with an acceptable regression coefficient of $R^2 = 0.95$ as shown in figure 4. The lower part of the graph in figure 4 shows the several parameters, which were determined by a MatLab routine from the measurement data and which represent the basic values for all further investigations and findings.

Measurement Results

Distribution of measurement data

As stated above, the down coming flow of the Pelton runner was measured over a rectangular area inside the casing. Therefore in the first step a validation was made, if these results gained for the rectangular area may be assigned / referred to the entire section of the casing. The first evaluation of the measurement data showed that the several parameters are distributed rotationally symmetrical with respect to the turbine axis TA (see figure 5 and 6).

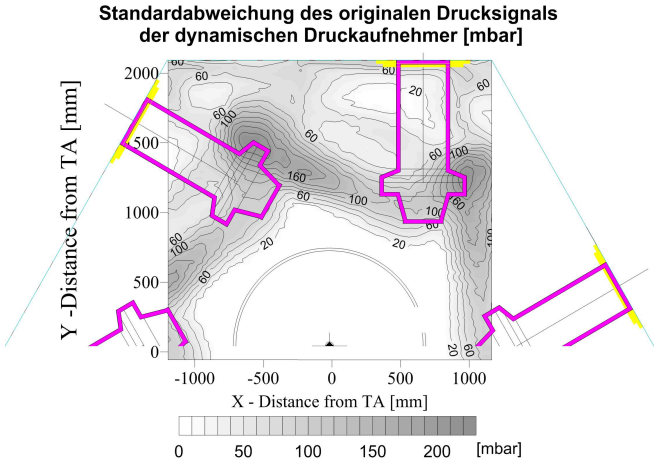

Figure 5: Standard deviation (root mean square) of the mode of the impact pressure signal

Thus the measurement values in the related triangular area were rotated step-by-step around the turbine axis by 60 degrees. This approach was validated by comparing the values from the original area with those from the entire casing section. Within this procedure a deviation of the values minor 1 % was detected and found acceptable.

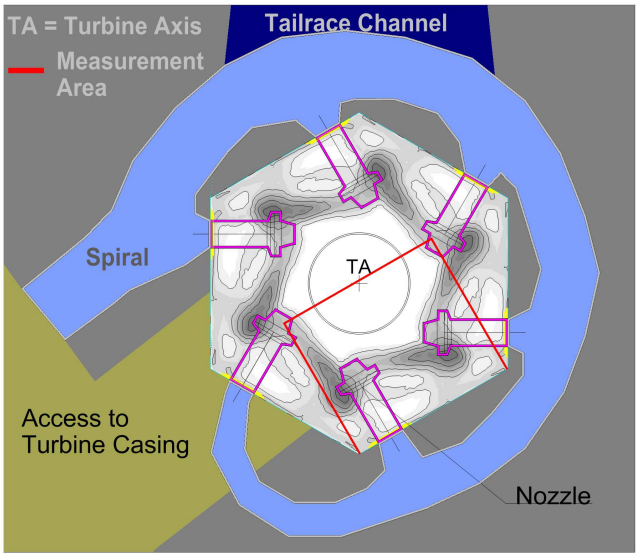

Figure 6: Orientation of the measurement area (1.95 m below the runner) and distribution of the standard deviation of the impact pressure signal rotated over the casing section

Impact velocity v_J

As it can be seen in figure 7, the maximal vertical impact velocity v_J is located directly below the buckets and is in the range of 10 to 11 m/s ($v_{J\,MAX}$ = 10.96 m/s).

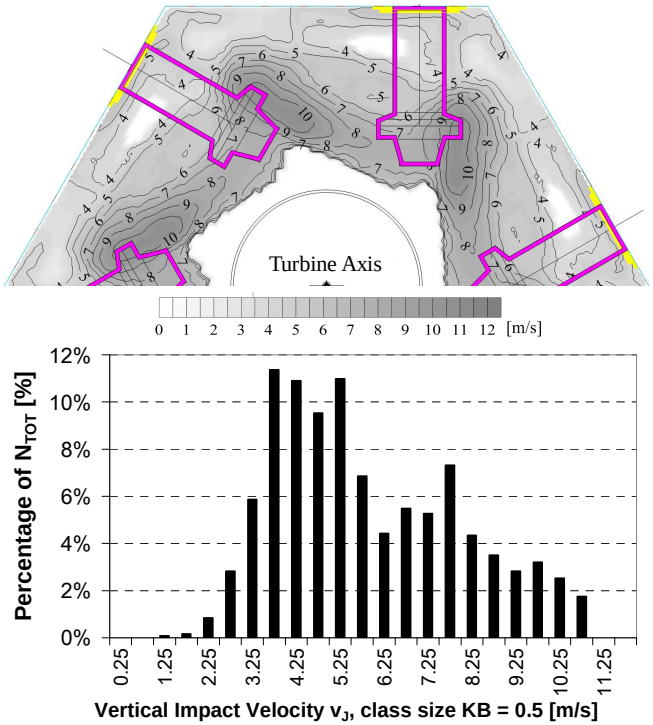

Figure 7: Distribution of the vertical impact velocity v_J

In this area the water flow coming out from the lower buckets is directly diverted to the tailrace channel without any major friction losses due to the interaction with the casing walls. The only interference for this water flow is the particle – particle interaction with the water flow dedicated to other buckets. In zones nearby the casing walls the velocity drops down to a level of 4 to 6 m/s.

These areas are dedicated to the flow coming from the upper buckets of the Pelton wheel which covers nearly the entire upper and lateral casing walls. The mean impact velocity was determined with $\overline{v_i}$ = 5.87 m/s which represents 5.07 % of the jet velocity at the nozzle v_{Nozzle} = 116 m/s. The mode of the velocity at the impact zone is 4.3 m/s.

The theoretical free fall velocity of a droplet related to the height difference between the runner plane and the measurement section is 6.18 m/s. Hence it can be stated that in the vicinity of the casing walls the flow is decelerated to a value lower than to the corresponding potential energy. It is assumed that the casing walls cause this decrease due to friction losses and the interaction of the several water shields inside the casing. In the region directly below the runner the measured velocities are about 60 % higher than the theoretical fall velocity. Therefore it is assumed that the interaction of the upper outflows from the Pelton runner with the casing walls has a major impact on the flow losses more than the interaction of the high energetic droplet layers directly below the runner.

Mean particle diameter D_T

Based on the vertical impact velocity and the parameters stated in figure 4 the mean particle diameter D_T can be calculated as follows:

$$D_T = v_J \cdot \overline{T_i} \qquad (4)$$

where $\overline{T_i}$ is the mean time of a particle hitting the probe counted from the first contact until the pressure value drops below a “noise” range of the signal which was set to 25 mbar.

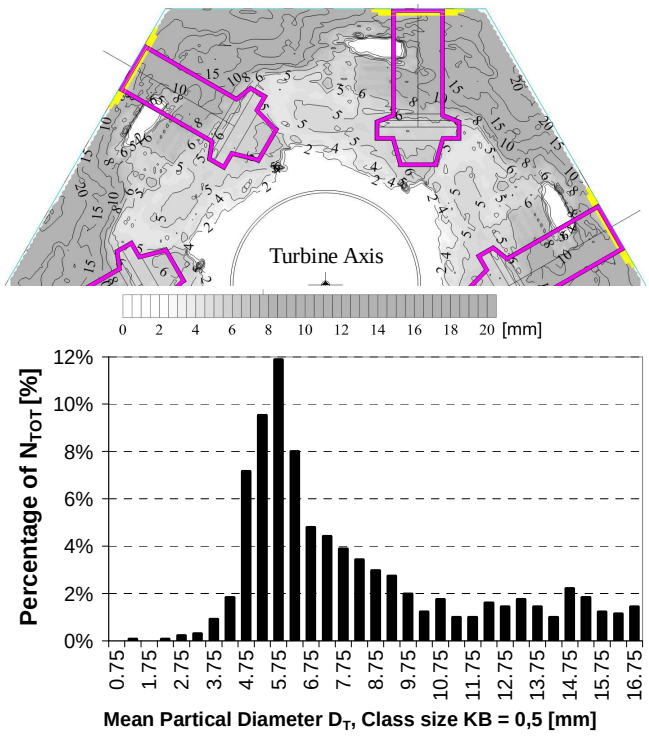

Figure 8: Distribution of the particle diameter D_T

As shown in figure 8, the range of the particle diameter in the inner circle is 5 to 6 mm. In zones with high velocities (10-11 m/s) the size of the water particles is found to be in the region of 5.2 to 5.3 mm.

In literature the maximal diameter of a stable, free falling water drop at the maximal velocity of app. 10 m/s is cited to be 5.26 mm, (Levich, 1962). In regions nearby the casing walls, larger diameters are calculated using equation (4) due to an accumulation of the water flows. Comparing figure 7 and figure 8 shows that these are the zones with lower velocities. The mode of the distribution of the particle diameter and thus the main-diameter is 5.32 mm (mean diameter $\overline{D_T}$ = 5.6 mm).

Discharge

Based on the known parameter, the discharge in each measuring point can be determined according to equation 5. The mean flow volume per reference area can be estimated using the mean droplet diameter and the numbers of particles hitting the transducer during the measurement. The size of the reference area of one pressure probe was 60.5 times 25 mm based on the distribution of the measurement points over the casing section.

$$q_E = N_T \cdot V_T \cdot n_{EF} \;,\; Q_{Tot} = \sum q_E \;\; with \;\; V_T = \pi \cdot \frac{D_T^3}{6} \qquad (5)$$

where q_E is the discharge per reference area, N_T the number of particles per second hitting the transducer (figure 9), n_{EF} the number of particles covering the reference area, V_T the volume of the particle in each reference area and D_T the referring mean particle diameter.

Summing up the discharges per reference area over the entire casing section yields the total discharge (figure 9). As only the vertical portion of the impact velocity was measured, the calculated total discharge had to be lower than the one measured at the penstock in the power house. To determine the number of particles over one reference area, the maximum number of droplets was calculated by assuming that each particle is in contact with the neighbouring one only at the surface based on the mean droplet diameter per reference area. Hence a total discharge was determined with Q_{TOT} = 6.27 m³/s, which is approximately 20 %, lower as that one measured at the penstock (Q_P = 7.56 m³/s). By dividing the casing section into two zones – the outer zone, which is the area directly at the casing walls up to a distance of 30 cm and the inner zone, which is represented by the remaining part of the casing section – it could be seen that based on this partition 55 % of the total discharge can be dedicated to the inner zone and thus to the outflow of the lower buckets and 45 % to the flow of the upper buckets. As a matter of fact, the flow of the lower and upper buckets is partitioned half /half, but it is interesting to mention that the flow of the upper buckets is referring only to 25 % of the entire casing area.

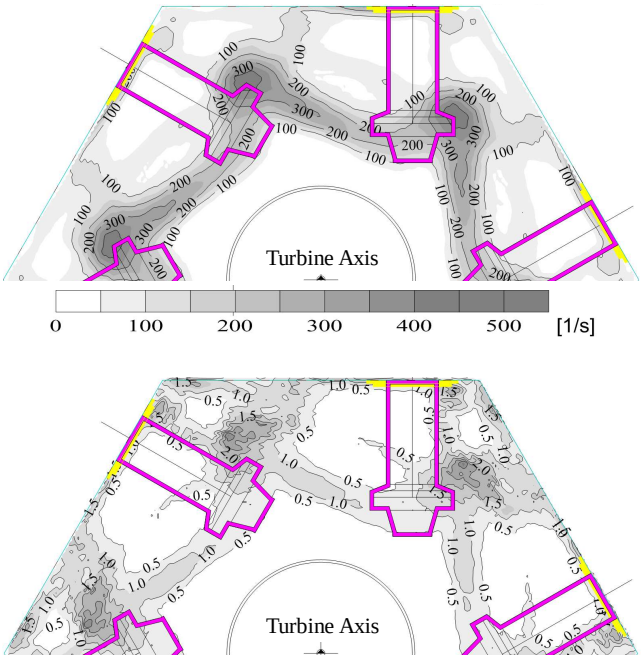

Figure 9: Distribution of drop impacts N_T per second (above) and distribution of the discharge per reference area (below)

Discussion

The geometrical dimensions and shape of the water particles is of major interest. Based on (Ryan, 1976) the maximum (terminal) fall velocity of a water droplet in air is 9.2 m/s. According to (Levich, 1962) critical diameters of water droplets flowing through gaseous media are in the range of 5.2 mm with a fall velocity of 8.0 m/s. Whether these particles are stable within their size or not can be determined by using the Weber number. Below the critical Weber number We < 12 free falling fluid particles are stable and no breakup occurs. If these particles are surrounded by turbulent flow fields, the critical Weber number is then reduced to We < 6.5, see (Pilch & Erdman, 1987) and (Clift, Grace, & Weber, 1978).

Based on the determined parameters, the Weber numbers for the particles were calculated according to the equation shown in the upper diagram of figure 10. As it can be seen, the major part of the water particles is below the critical Weber number We = 6.5. This means that most of the particles are stable and will not break apart any longer. In the vicinity of the casing walls the flow from the ceiling is accumulated and so are the particles too. Therefore – as it can be seen in figure 8 – the remaining 20 % are representing this portion of the flow dedicated to the outflow of the upper buckets.

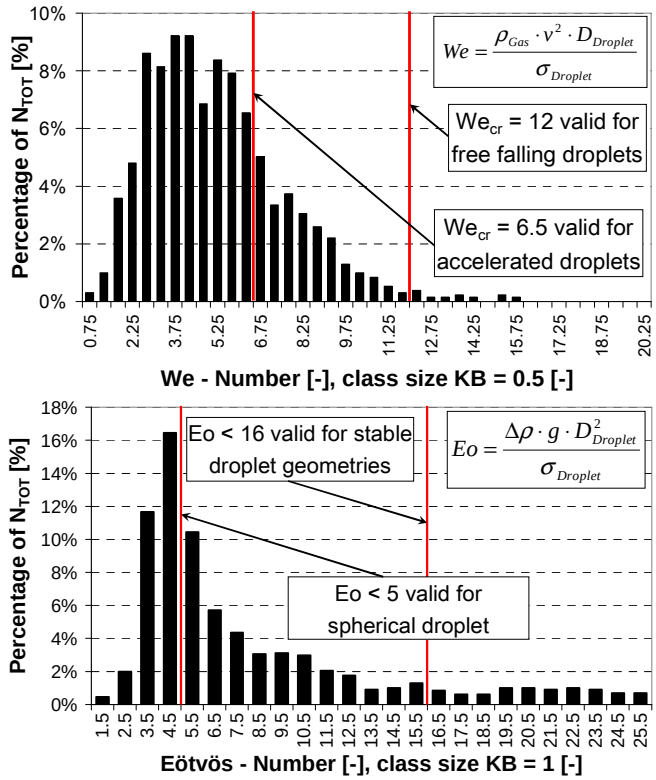

Figure 10: Distribution of Weber number *We* (above) and Eotvös number *Eo* (below) where ρ_{Gas} is the density of the ambient gas (in this case air), ν is the kinematic viscosity of the fluid, σ is the surface tension of the liquid and $\Delta\rho$ is the difference in density of the liquid and gas-phase.

Besides the Weber number the Eotvös number is representative for the stability and shape of a droplet. As stated above, the layer of the water film directly at the outer edge of the bucket is in the range of 17 to 25 mm. This means according to the presented particle diameters that the water layer is 3 to 6 times larger than the particles hitting the tailrace water level. In the zones of higher velocities $Eo > 5$ is not exceeded. This means according to the distribution of the Eotvös number that approximately 34 % of the flow coming down from the Pelton runner is in the form of stable spherical water droplets, 75 % of the flow is in the range $Eo < 16$. The remaining part of 25 % of the flow is on the one hand still in the process of droplet break-up and on the other hand this part is also dedicated to accumulating particles in the wall region. Nevertheless it can be assumed that the major part of the flow hitting the tail water surface consists of more or less spherical particles.

Conclusion

The paper describes results of prototype measurements on the distribution of the flow just above the tailrace water level coming down from a vertical Pelton wheel. Measurement data were gathered by using a newly developed measuring technique based on pressure probes.

Flow coming from the buckets splits up to droplets which either fall down on the tailwater freely or flow along the casing wall towards the tailwater.

The maximal vertical impact velocity v_J of droplets is located directly below the lower buckets and is in the range of 10 to 11 m/s. In zones nearby the casing walls the velocity drops down to a level of 4 to 6 m/s.

In zones with high velocities (10-11 m/s) the diameter of the water particles is found to be in the range of 5.2 to 5.3 mm. In regions nearby the casing walls, larger diameters > 10 mm were calculated due to an accumulation of the water flow.

Acknowledgments

The studies described in this paper were possible only due to financial support from the Austrian Federal Ministry of Economy, Family and Youth and VEÖ (Verband Elektrizitätsunternehmen Österreich). Moreover, these investigations could be realized with the outstanding help & support of Kelag power utility, which made staff available and permitted restrictions on the operation of their plant during measurements.

References

Arch, A. (2008). *Luftein- und Austragsprozesse bei Anlagen mit Peltonturbinen im Gegendruckbetrieb.* Schriftenreihe zur Wasserwirtschaft - Vol.52: Technische Universität Graz.

Arch, A., & Mayr, D. (14 - 2 2006). De-aeration of air-water flows in the tailwater channels of Pelton turbines. *The international Journal of Hydropower & Dams*, S. 106 - 110.

Arch, A., & Mayr, D. (2006). *Hydro-power plant equipped with Pelton turbines: Basic experiments relating to the influence of backpressure on the design.* Southampton: WIT Press.

Clift, R., Grace, J. R., & Weber, M. E. (1978). *Bubbles, Drops and Particles.* Academic Press.

Levich, V. G. (1962). *Physicochemical Hydrodynamics.* Prentice-Hall International Series.

Pilch, M., & Erdman, C. (Issue 6. Vol. 13 1987). Use of Breakup Time Data and Velocity History Data to predict the Maximum Size of Stable Fragments for Acceleration-Induced Breakup of a Liquid Drop. *Int. J. of Multiphase Flows*, 741-757.

Ryan, R. (Vol. 15 1976). The Behaviour of large, low-Surface-Tension Water Drops falling at terminal Velocity in Air. *Journal of Applied Meterology*, 157-165.